Am J Physiol Cell Physiol 290: C1146–C1159, 2006.
First published November 23, 2005; doi:10.1152/ajpcell.00205.2005.

TRPM2 is an ion channel that modulates hematopoietic cell death through activation of caspases and PARP cleavage

Wenyi Zhang,[1] Iwona Hirschler-Laszkiewicz,[1] Qin Tong,[1] Kathleen Conrad,[1] Shao-Cong Sun,[2] Linda Penn,[6] Dwayne L. Barber,[6] Richard Stahl,[7] David J. Carey,[7] Joseph Y. Cheung,[3,4] and Barbara A. Miller[1,5]

Departments of [1]Pediatrics, [2]Microbiology and Immunology, [3]Cellular and Molecular Physiology, [4]Medicine, and [5]Biochemistry and Molecular Biology, The Pennsylvania State University College of Medicine, Hershey, Pennsylvania; [6]Division of Cellular and Molecular Biology, Ontario Cancer Institute, Toronto, Ontario, Canada; and [7]Sigfried and Janet Weis Center for Research, Geisinger Clinic, Danville, Pennsylvania

Submitted 28 April 2005; accepted in final form 18 November 2005

Zhang, Wenyi, Iwona Hirschler-Laszkiewicz, Qin Tong, Kathleen Conrad, Shao-Cong Sun, Linda Penn, Dwayne L. Barber, Richard Stahl, David J. Carey, Joseph Y. Cheung, and Barbara A. Miller. TRPM2 is an ion channel that modulates hematopoietic cell death through activation of caspases and PARP cleavage. *Am J Physiol Cell Physiol* 290: C1146–C1159, 2006. First published November 23, 2005; doi:10.1152/ajpcell.00205.2005.—TRPM2 is a Ca^{2+}-permeable channel activated by oxidative stress or TNF-α, and TRPM2 activation confers susceptibility to cell death. The mechanisms were examined here in human monocytic U937-ecoR cells. This cell line expresses full-length TRPM2 (TRPM2-L) and several isoforms including a short splice variant lacking the Ca^{2+}-permeable pore region (TRPM2-S), which functions as a dominant negative. Treatment with H_2O_2, a model of oxidative stress, or TNF-α results in reduced cell viability. Expression of TRPM2-L and TRPM2-S was modulated by retroviral infection. U937-ecoR cells expressing increased levels of TRPM2-L were treated with H_2O_2 or TNF-α, and these cells exhibited significantly increased intracellular calcium concentration ($[Ca^{2+}]_i$), decreased viability, and increased apoptosis. A dramatic increase in cleavage of caspases-8, -9, -3, and -7 and poly(ADP-ribose)polymerase (PARP) was observed, demonstrating a downstream mechanism through which cell death is mediated. Bcl-2 levels were unchanged. Inhibition of the $[Ca^{2+}]_i$ rise with the intracellular Ca^{2+} chelator BAPTA blocked caspase/PARP cleavage and cell death induced after activation of TRPM2-L, demonstrating the critical role of $[Ca^{2+}]_i$ in mediating these effects. Downregulation of endogenous TRPM2 by RNA interference or increased expression of TRPM2-S inhibited the rise in $[Ca^{2+}]_i$, enhanced cell viability, and reduced numbers of apoptotic cells after exposure to oxidative stress or TNF-α, demonstrating the physiological importance of TRPM2. Our data show that one mechanism through which oxidative stress or TNF-α mediates cell death is activation of TRPM2, resulting in increased $[Ca^{2+}]_i$, followed by caspase activation and PARP cleavage. Inhibition of TRPM2-L function by reduction in TRPM2 levels, interaction with TRPM2-S, or Ca^{2+} chelation antagonizes this important cell death pathway.

oxidative stress; tumor necrosis factor-α; apoptosis

TRPM2 IS A MEMBER of the transient receptor potential (TRP) channel superfamily, a diverse group of Ca^{2+}-permeable cation channels expressed on nonexcitable cells and related to the archetypal *Drosophila* TRP (9, 17, 29). The TRP superfamily, conserved from *Caenorhabditis elegans* to humans, has been divided into seven subfamilies designated C, V, M, A, N, P, and ML (2, 29). Mammalian isoforms have six putative transmembrane domains and a putative pore loop between the fifth and sixth transmembrane domains. They are voltage independent and are proposed to function as tetramers. A number of important physiological processes including vasoactivation, sensation, fertility, and cell proliferation involve members of the TRP family (9). One subfamily of TRP channels has been designated the TRPM family, named after the first described member, melastatin, a putative tumor suppressor protein (11, 29, 30). TRPM1 is expressed on melanocytes, and its expression level correlates inversely with melanoma aggressiveness and the potential for metastasis (11, 20). Several other TRPM members may have important roles in cell proliferation, including TRPM2 (16, 47), TRPM5 (38), TRPM7 (1), and TRPM8 (42).

TRPM2, also called LTRPC-2 or TRPC7, was the second member of the TRPM subfamily to be described (31, 39). TRPM2 has been cloned from human brain, lymphocytes, monocytes, and bone marrow (31, 34, 39, 47) and is expressed in many cell types including brain, hematopoietic cells, and the gastrointestinal tract (39). TRPM2 channels are permeable to Na^+, K^+, and Ca^{2+} and are activated by several second messengers (35, 39). Intracellular ADP-ribose (ADPR) activates TRPM2 by binding to the TRPM2 COOH-terminal NUDT9-H domain, which has significant homology with NUDT9 ADP-ribose hydrolase (18, 23, 24, 35, 43). NAD has been reported to directly activate TRPM2 (16, 39), but the predominance of evidence suggests that NAD activates TRPM2 through conversion to ADPR (35, 36, 43). Intracellular Ca^{2+} further sensitizes cells to gating by ADPR (27). Extracellular signals that activate TRPM2 include oxidant stress, application of H_2O_2, and TNF-α (16, 43). Whether these stimuli activate TRPM2 directly through production of second messengers such as ADPR or through unidentified mechanisms is currently under investigation.

In addition to full-length TRPM2 (TRPM2-L), three physiological TRPM2 splice variants have been identified in human hematopoietic cells: TRPM2-S (47), TRPM2-ΔN (43), and TRPM2-ΔC (43). TRPM2-S (short) has a deletion of the entire COOH terminus, including four of six COOH-terminal transmembrane domains and the putative Ca^{2+}-permeable pore, and functions to inhibit TRPM2-L activity (47). TRPM2-ΔN has a

Address for reprint requests and other correspondence: B. A. Miller, Dept. of Pediatrics, Milton S. Hershey Medical Center, PO Box 850, Hershey, PA 17033 (e-mail: bmiller3@psu.edu).

The costs of publication of this article were defrayed in part by the payment of page charges. The article must therefore be hereby marked "*advertisement*" in accordance with 18 U.S.C. Section 1734 solely to indicate this fact.

deletion of amino acids 538–557 in the NH_2 terminus. HEK 293 cells expressing TRPM2-ΔN fail to respond to H_2O_2 or ADPR, suggesting that the TRPM2-ΔN mutation dominantly disrupts channel gating, channel assembly, or surface trafficking (43). TRPM2-ΔC has a deletion of amino acids 1292–1325 in the COOH-terminal CAP domain of NUDT9-H, decreasing affinity for ADPR (43). HEK 293 cells expressing TRPM2-ΔC respond to H_2O_2 but not to intracellular application of ADPR, suggesting that oxidative stress may activate TRPM2 through a mechanism independent of ADPR. The role of the latter two splice variants in susceptibility to cell death is not known.

Here we examined the mechanism through which TRPM2 induces death after cells are exposed to oxidative stress or TNF-α. We used a subclone of the human monocytic cell line U937 that was stably transfected with an ecotropic retroviral receptor (U937-ecoR). This cell line endogenously expresses TRPM2-L and TRPM2-S and is susceptible to cell death induced by H_2O_2 or TNF-α (15). To confirm the function of TRPM2 in this cell line, expression of TRPM2-L was modulated by retroviral infection. Treatment of cells expressing increased TRPM2-L with H_2O_2 or TNF-α resulted in increased intracellular Ca^{2+} concentration ($[Ca^{2+}]_i$) and numbers of apoptotic cells, and cell viability was reduced. The mechanism leading to induction of cell death involved increased cleavage of procaspases-8, -9, -7, and -3, as well as poly(ADP-ribose) polymerase (PARP). Inhibition of the rise in $[Ca^{2+}]_i$ with the intracellular Ca^{2+} chelator BAPTA blocked caspase activation and PARP inactivation, demonstrating that this cell death pathway requires a rise in $[Ca^{2+}]_i$. Increased expression of TRPM2-S blocked the rise in $[Ca^{2+}]_i$ in response to H_2O_2 or TNF-α and enhanced cell survival, consistent with the role of TRPM2-S as an inhibitor of endogenous TRPM2-L activity (47). Downregulation of endogenous TRPM2-L with RNA interference (RNAi) confirmed the physiological role of TRPM2 in susceptibility of cells to death.

EXPERIMENTAL PROCEDURES

Culture of cell lines and human BFU-E-derived cells. Jurkat, K562, and AML-193 cells were obtained from and cultured under conditions recommended by the American Type Culture Collection (Manassas, VA). 293T cells were cultured in DMEM with 10% FBS. U937-ecoR cells, a cell line stably expressing ecotropic receptor for retrovirus and generated in the laboratory of L. Penn, were cultured in α-MEM with 10% FBS. Peripheral blood from volunteer donors was obtained under protocols approved by the Pennsylvania State University College of Medicine and Geisinger Clinic Institutional Review Boards. Human BFU-E were cultured, and BFU-E-derived erythroblasts were harvested as described previously (46).

RT-PCR of TRPM2 splice variants in human primary cells and cell lines. RNA was prepared from human cell lines and BFU-E-derived erythroblasts. RNA from $CD34^+$ cells and fresh monocytes was purchased from AllCells (Foster City, CA). cDNA was prepared from RNA with the Superscript first-strand synthesis system (Invitrogen, Carlsbad, CA). RT-PCR was routinely performed for 35 cycles (denaturation at 94°C for 30 s, annealing and extension at 68°C for 3 min). RT-PCR of GAPDH was performed for only 25 cycles. A set of primers was identified that specifically recognized the TRPM2-S isoform: 5′ primer, 5′-TGTGCGAGGAGATGCGGCAGTAG-3′; 3′ primer, 5′-CAGGATGTTGGTGAAGAGCAGGTA-3′. Primers used to document expression of all TRPM2 isoforms were 5′ primer, 5′-TCGGACCCAACCACACGCTGTA-3′; 3′ primer, 5′-CGTCATTCTGGTCCTGGAAGTG-3′. Primers used to detect expression of TRPM2-ΔC and TRPM2-ΔN isoforms were described previously (43). Primers used to document expression of TRPM2 isoforms after retroviral infection with pCLXSN-GFP were TRPM2 (L/S): 5′ primer, 5′-TCCCTCTACAAGCGTTCCTCAG-3′ (no. 129), 3′ primer, 5′-TCCTCCTTGGACAGCTCCTTCAG-3′(no. 128); and TRPM2-S: 5′ primer (no. 129), 3′ primer, 5′-TAGAAGGCACAGTCGAGG-3′ (no. 187, in pCLXSN vector). Primer 187 recognizes a sequence in the BGH reverse priming site, which is present in pCLXSN vector as a result of subcloning the TRPM2-S fragment from the pcDNA3.1/V5-His-TOPO vector. Control GAPDH primers used in RT-PCR were 5′ primer, 5′-ATGACCACAGTCCATGCCATCACTG-3′; 3′ primer; 5′-GGTCTTACTCCTTGGAGGCCATGT-3′. Control 18S rRNA primers were reported previously (47). Primers to document expression of the pSuppressorRetro Vector Neo gene were 5′ primer, 5′-CTTGCTCCTGCCGAGAAAGT-3′; 3′ primer, 5′-TTCGCTTGGTGGTCGAATG-3′.

Overexpression of TRPM2 with retroviral infection. The retroviral vector pCLXSN was modified to express green fluorescent protein (GFP) from the SV40 promoter. TRPM2 isoforms TRPM2-S and TRPM2-L were subcloned into pCLXSN-GFP and expressed from the cytomegalovirus (CMV) promoter. Retroviral pCLXSN vector with or without TRPM2 isoforms was packaged by transfecting 293T cells, using Fugene6 with pCLXSN, pCL-Eco (Imgenex, San Diego CA), and cmv.G encoding VSV glycoprotein (32). Twenty-four hours after transfection, the medium was removed and replaced with DMEM. Forty-eight hours after transfection, the viral supernatant was harvested and filtered. U937-ecoR cells were infected by spinning 1×10^6 cells with the viral supernatant in six-well plates at 1,800 rpm for 45 min at room temperature with 8 μg/ml polybrene, followed by incubation at 37°C. At 24 h after infection, the viral supernatant was removed and cells were washed. Seventy-two hours after infection GFP fluorescence was determined to assess infection efficiency, and cells were used in proliferation and survival experiments.

Immunolocalization of TRPM2 in U937-ecoR cells. U937-ecoR cells were placed in wells of Lab-Tek Permanox chamber slides precoated with fibronectin. After 2 h, cells were washed three times with PBS, fixed with paraformaldehyde, and permeabilized in 0.05% Triton X-100 in PBS for 2 min on ice. After being washed three times, cells were stained with primary antibody (1:50) in 5% milk in Tris-buffered saline for 1 h at room temperature. Anti-TRPM2-N recognizes TRPM2-S and TRPM2-L, and anti-TRPM2-C recognizes only TRPM2-L (47). Anti-TRPM2-C antibody was used to document localization of endogenous and retrovirus-expressed TRPM2-L in U937-ecoR cells. Slides were stained with secondary goat anti-rabbit Alexa 488 Fluor (Molecular Probes, Eugene, OR; 1:200) or donkey anti-rabbit rhodamine red (ImmunoResearch Laboratories, West Grove, PA; 1:200) for 30 min in the dark. To detect retrovirus-infected TRPM2-S, cells were stained with anti-V5 (Invitrogen; 1:200) and secondary donkey anti-mouse Cy5 antibody (ImmunoResearch Laboratories; 1:200). Coverslips were mounted with Vectashield mounting medium with or without 4′,6-diamidino-2-phenylindole dihydrochloride (DAPI) or propidium iodide (Vector Laboratories, Burlingame, CA). Images were acquired with a Leica TCS SP2 confocal microscope or with a Nikon Eclipse TE2000 microscope equipped for epifluorescence.

Immunoblotting of whole cell lysates. For Western blot analysis, whole cell lysates were separated on 8% polyacrylamide gels, followed by transfer to Hybond-C Extra membranes (Amersham Biosciences, Piscataway, NJ). Blots were incubated with anti-TRPM2-N (1:250) (47), anti-TRPM2-C (1:300) (47), anti-TRPC6 (1:200; Alomone Laboratories, Jerusalem, Israel), anti-actin (1:750; Sigma, St. Louis, MO), anti-GFP (1:500; Santa Cruz Biotechnology, Santa Cruz, CA), anti-caspase-8 (1:1,000; R&D Systems, Minneapolis, MN), anti-caspase-9 (1:1,000; no. 9502, Cell Signaling Technology, Beverly, MA), anti-caspase-3 (1:1,000; no. 9662, Cell Signaling Technology), anti-caspase-7 (1:1,000; no. 9492, Cell Signaling Technology), anti-PARP (1:1,000; no. 9542, Cell Signaling Technology), and anti-Bcl-2 (1 μg/ml; BD Biosciences Pharmingen, San Diego,

CA) antibodies. Blots were washed and incubated with the appropriate horseradish peroxidase-conjugated antibodies (1:2,000). Enhanced chemiluminescence was used for detection of signal. For the Western blots shown in Figs. 2*C* and 8*C*, lysates were treated at 60°C for 30 min before loading, instead of boiling for 10 min, to prevent aggregation before gel entry that has been reported for membrane proteins (14). This allowed detection of endogenous TRPM2 protein.

Measurement of $[Ca^{2+}]_i$ with digital video imaging. U937-ecoR cells were infected with the empty pCLXSN vector or with pCLXSN into which TRPM2-L or TRPM2-S was subcloned. Successful infection of single U937-ecoR cells with pCLXSN vector was verified by detection of GFP (excitation 478 nm, emission 535 nm) with our fluorescence microscopy-coupled digital video imaging system (6, 7, 28). To study changes in $[Ca^{2+}]_i$ in infected cells, we were not able to use fura-2 as the detection fluorophore because its excitation and emission wavelengths overlap with GFP. Instead, we used the fluorescent indicator Fura Red (excitation 440 and 490 nm, emission 600 nm long pass), a dual-wavelength excitation probe (25, 44). At 3–5 days after infection, U937-ecoR cells attached to fibronectin-coated glass coverslips were loaded with 5 μM Fura Red-AM for 20 min at 37°C in the presence of Pluronic F-127. The extracellular buffer routinely contained 0.68 mM $CaCl_2$. In experiments to examine the role of extracellular Ca^{2+} influx, cells were studied in extracellular buffer with 2 mM EGTA without Ca^{2+}. In experiments to inhibit the rise in $[Ca^{2+}]_i$, cells were pretreated for 60 min with the cell-permeant intracellular Ca^{2+} chelator BAPTA-AM (10 μM; Molecular Probes). U937-ecoR cells were then treated with 0 or 1 mM H_2O_2 or 100 ng/ml TNF-α. $[Ca^{2+}]_i$ was measured in individual cells at baseline and over a 20-min interval by determination of the fluorescence intensity ratio (R, F_{440}/F_{490}). In experiments to determine the time course of the rise in $[Ca^{2+}]_i$, measurements were obtained at 5-s intervals for the first 30 s, 15-s intervals for the next 90 s, and then 2- to 5-min intervals to 20 min. $[Ca^{2+}]_i$ was calculated with the formula $[Ca^{2+}]_i = K'_D[(R - R_{min})/(R_{max} - R)](S_{f2}/S_{b2})$, where R_{min} and R_{max} are minimum and maximum R, respectively, after calibration of S_{f2}/S_{b2} is the ratio of fluorescence proportionality coefficient obtained at 490 nm excitation under R_{min} (S_{f2}) and R_{max} (S_{b2}) conditions and K'_D is the apparent Ca^{2+} Fura red dissociation constant, as described previously (8).

Assays of cell viability. Cell viability was assessed by Trypan blue exclusion. Proliferation was assessed with the CellTiter 96 AQ_{ueous} One Solution cell proliferation assay (Promega, Madison, WI), which uses 3-(4,5-dimethylthiazol-2-yl)-5-(3-carboxymethoxyphenyl)-2-(4-sulfophenyl)-2*H*-tetrazolium, inner salt (MTS). Apoptosis was also assessed with Vibrant Apoptosis Assay Kit no. 2 (Molecular Probes). Apoptotic cells were labeled with annexin V conjugated to Alexa Fluor 488 or 594 and detected by fluorescence microscopy.

Flow cytometric analysis for detection of apoptotic cells. Annexin V-PE Apoptosis Detection Kit I (BD Biosciences) was used to detect apoptotic and dead cells based on the manufacturer's protocols. Cells were stained with annexin V-PE to detect phosphatidylserine externalized on the surface of apoptotic cells and with 7-amino-actinomycin (AAD) to identify nonviable cells, followed by flow cytometry. Cells that are annexin V-PE^- and 7-AAD^- are alive and not undergoing measurable apoptosis, cells that are annexin V-PE^+ and 7-AAD^- are in early apoptosis, and cells that are annexin V-PE^+ and 7-AAD^+ are in late apoptosis or necrosis or are dead.

Downregulation of TRPM2 by RNA interference. A vector (pSUPER) was prepared by modification of pCMV-Script; the fragment between the *Vsp*I and *Mlu*I sites was removed and replaced with the H1 RNA polymerase promoter. Three oligonucleotide sequences for generation of hairpin RNAs that target three different TRPM2 sites were designed as templates. The sequences of these three oligonucleotides, based on the TRPM2 sequence (GenBank Accession no. AB001535) were *1*) nucleotides 508–526, CAGAAGGGTCACTGACCTGTTCAAGAGACAGGTCAGTGACCCTTCTG; *2*) nucleotides 539–561, AATCTCCGGCGCAGCAACAGCAGTTCAAGAGACTGCTGTTGCTGCGCCGGAGATTT; and *3*) nucleotides 612–632, AAGAAAGCCTCAGTTCGTGGATTCAAGAGATCCACGAACTGAGGCTTTCTTT. Sequences complementary to the M13 forward (CAGGAAACAGCTATGACGGATCC) and reverse (TTTTTAAGCTTCTGGCCGTCGTTTTAC) primers were added to the 5′ or 3′ ends, respectively, during oligonucleotide synthesis. M13 forward and reverse primers were used to amplify these three DNA fragments, and the PCR products were first cloned into the PCR2.1-TOPO TA vector and then subcloned into pSUPER by using *BamH*I and *Hind*III sites, respectively. These small interfering (siRNA) constructs in pSuper were used to transfect 293T cells to determine the most effective siRNA construct for use in U937-ecoR cells.

The retroviral vector pSuppressorRetro (Imgenex, San Diego, CA) was used to infect U937-ecoR cells. Oligonucleotides for generation of hairpin RNA in cells were designed based on the manufacturer's recommendations. RNAi targeted to TRPM2 nucleotides 612–632 was used in these experiments, and RNAi targeted to luciferase was used as a negative control. The sequences of the double-stranded oligonucleotides used to create TRPM2 siRNA are 5′-TCGAAAGAAAGCCTCAGTTCGTGGAttcaagagaTCCACGAACTGAGGCTTTCTTTTTT-3′ and 5′-CTAGAAAAAAAGAAAGCCTCAGTTCGTGGAtctcttgaaTCCACGAACTGAGGCTTTCTT-3′; the *Xho*I and *Xba*I sites, respectively, are underlined. For siRNA targeted to luciferase, the sequences are 5′-TCGAAACGTACGCGGAATACTTCGATTttcaagagaAATCGAAGTATTCCGCGTACGTTTTTTT-3′ and 5′-CTAGAAAAAAACGTACGCGGAATACTTCGATTtctcttgaaAATCGAAGTATTCCGCGTACGTT-3′ (12). Two oligonucleotides for each RNAi were annealed in vitro and then inserted into linearized vector pSuppressorRetro. Recombinant pSuppressorRetro was packaged by transfecting 293 T cells with Fugene6 with pCL-Eco and cmv.G encoding VSV glycoprotein (32). U937-ecoR cells were infected as described above.

Statistics. All results are means ± SE. Statistical significance was determined by unpaired Student's *t*-test or by one-way analysis of variance.

RESULTS

Expression of TRPM2 in human hematopoietic cell lines and primary cells. TRPM2 expression has been demonstrated in lymphocytes, granulocytes, and hematopoietic cell lines by RT-PCR (18, 39, 43, 47). To examine the expression and function of TRPM2 in hematopoietic cells, selected as a model for other lineage-committed cells (39), RT-PCR was performed with RNA isolated from Jurkat (T cell lymphoblast), K562 (chronic myelogenous leukemia), AML-193 (acute monocytic leukemia), and U937-ecoR (monocytic leukemia) cell lines. RNA was also isolated from primary human hematopoietic cells at different stages of maturation, including $CD34^+$ progenitor cells purified from human bone marrow, monocytes enriched from human peripheral blood ($CD14^+$), and erythroblasts harvested at day 10 of culture of human peripheral blood erythroid progenitors (BFU-E) (45). Expression levels of TRPM2 isoforms were equalized by comparison to GAPDH expression. TRPM2, detected by primers that recognize all isoforms, was highly expressed in Jurkat, K562, AML-193, and U937-ecoR cells and in primary $CD34^+$ cells and monocytes (Fig. 1*A*). Expression of the TRPM2-S, TRPM2-ΔC, and TRPM2-ΔN splice variants was studied with specific primers for each isoform. RNAs for TRPM2-S and TRPM2-ΔC but not TRPM2-ΔN were detected in U937-ecoR cells. Expression of endogenous TRPM2 protein was examined in U937-ecoR cells with confocal microscopy (Fig. 1*B*). Immunofluorescence demonstrated expression of endogenous TRPM2 at or near the cell membrane of U937-ecoR cells.

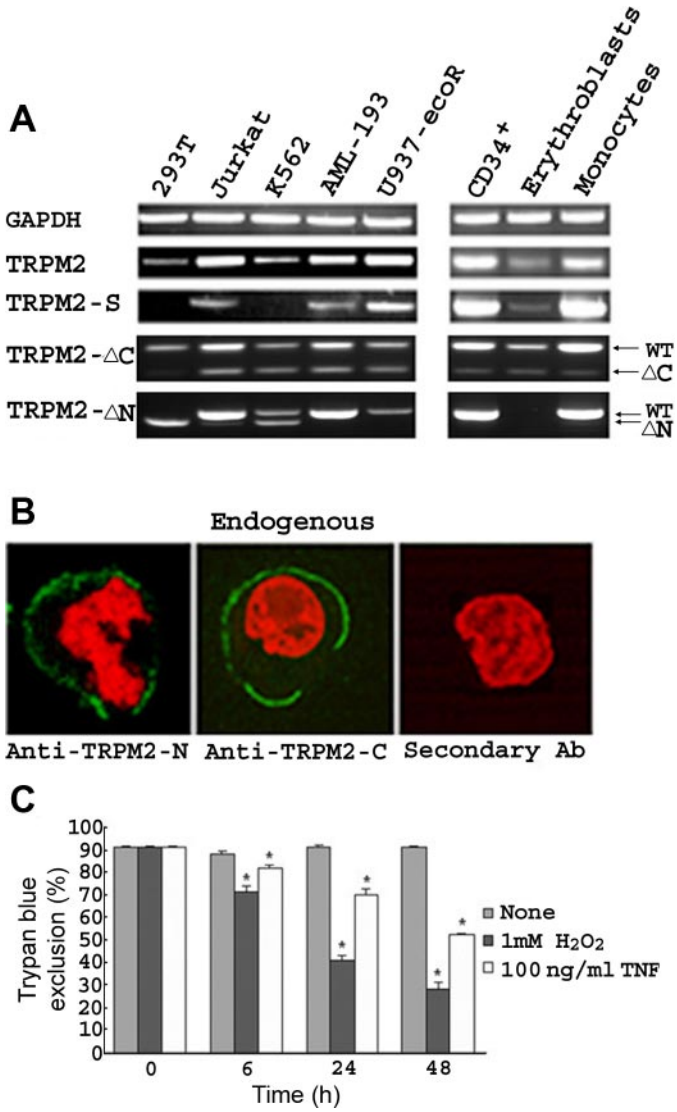

Fig. 1. Endogenous expression of TRPM2 in human hematopoietic cells. *A*: RT-PCR was performed on RNA isolated from 293T, Jurkat, K562, AML-193, and U937-ecoR cell lines and from primary CD34$^+$ cells, BFU-E derived erythroblasts at *day 10* of differentiation, and peripheral blood monocytes. Primers specifically identified TRPM2, variants TRPM2-S, TRPM2-ΔC, and TRPM2-ΔN, and GAPDH. RT-PCR was performed twice with similar results. WT, wild type. *B*: localization of endogenous TRPM2 in U937-ecoR cells was determined by immunofluorescence with confocal microscopy after staining with anti-TRPM2-N or anti-TRPM2-C antibodies or nonspecific serum and with goat anti-rabbit Alexa 488 secondary antibody. A representative result of 3 similar experiments is shown. *C*: U937-ecoR cells were treated with 0 or 1 mM H_2O_2 or 100 ng/ml TNF-α, and cell viability was assessed by Trypan blue exclusion at 0, 6, 24, and 48 h after treatment. *Cell viability was significantly reduced in a time-dependent manner after 6, 24, and 48 h of treatment with H_2O_2 or TNF-α ($P < 0.03$, $P < 0.001$, $P < 0.0001$, respectively). Results shown are representative of 4 experiments.

Susceptibility of U937-ecoR cells to death induced by oxidative stress or TNF-α. The susceptibility of U937-ecoR cells to death was examined by treating them with 1 mM H_2O_2, a model of oxidative stress, or with 100 ng/ml TNF-α. This resulted in a significant and time-dependent decrease in cell viability, measured by Trypan blue exclusion (Fig. 1*C*), that was statistically significant at 6 h. At 24 and 48 h, further decreases in cell viability were observed.

TRPM2-L enhances and TRPM2-S suppresses susceptibility to cell death induced by H_2O_2 or TNF-α. The role of TRPM2-L and TRPM2-S in cell death induced by H_2O_2 and TNF-α in U937-ecoR cells was determined before examining the mechanism. TRPM2-S rather than TRPM2-ΔC was selected for study because of its function as a dominant-negative isoform (47). To modulate expression levels, U937-ecoR cells were infected with the empty retroviral vector pCLXSN-GFP or pCLXSN-GFP expressing TRPM2-L or TRPM2-S. GFP fluorescence was observed in the majority of cells (Fig. 2*A*), demonstrating the high infection efficiency. Although GFP fluorescence was routinely greater in TRPM2-L- than TRPM2-S-expressing cells, excellent expression of TRPM2-L or TRPM2-S was documented by both RT-PCR and Western blotting (Fig. 2, *B* and *C*). No PCR bands were detected without the reverse transcriptase step, demonstrating the specificity of the RT reaction (Fig. 2*B*, *panel 1*, *lanes 1–3*). Endogenous TRPM2 expression was detected in U937-ecoR cells with primers that recognize both TRPM2-L and TRPM2-S (Fig. 2*B*, *panel 2*, *lane 1*, nos. 129, 128). RT-PCR confirmed increased heterologous expression of TRPM2-L and TRPM2-S (Fig. 2*B*, *panel 2*, *lanes 2* and *3*) and TRPM2-S (Fig. 2*B*, *panel 3*, *lane 3*). The quality of RNA preparations was demonstrated with primers for 18S rRNA (Fig. 2*B*, *4th panel*, *lanes 1–3*). Western blot analysis demonstrated increased expression of TRPM2-L (171 kDa) or TRPM2-S (95 kDa) protein in infected U937-ecoR cells (Fig. 2*C*) compared with endogenous levels. The Western blots shown in Fig. 2*C* were probed with anti-GFP antibody and showed highest expression of GFP in cells infected by empty vector, with less expression in cells infected with vector also expressing TRPM2-L or TRPM2-S, consistent with the immunofluorescence studies in Fig. 2*A*. Although lower expression of GFP was observed in all experiments in cells infected with pCLXSN expressing TRPM2-S, three different experiments showed excellent TRPM2-S protein expression by Western blot analysis. Expression of retrovirus-expressed TRPM2-L and TRPM2-S at or near the plasma membrane, as well as in the cytoplasm, was confirmed by immunofluorescence and confocal microscopy (Fig. 2*D*).

The proliferation of U937-ecoR cells was examined in cells expressing increased levels of TRPM2-L or TRPM2-S by measurement of MTS tetrazolium bioreduction (Fig. 3*A*). Even without treatment, a significantly lower level of activity was detected in cells expressing TRPM2-L compared with cells infected with empty vector ($P < 0.003$). The proliferation of cells expressing TRPM2-S was significantly higher than that of cells expressing TRPM2-L ($P < 0.0001$). The proliferation of cells expressing TRPM2-S was greater than that of cells expressing empty vector, but this did not reach statistical significance in the absence of stress or a negative stimulus.

The ability of TRPM2-L or TRPM2-S to modulate cell death induced by oxidative stress (H_2O_2) or TNF-α was then determined. At 72 h after infection with empty pCLXSN retroviral vector or virus expressing TRPM2-L or TRPM2-S, U937-ecoR cells were treated with 0 or 1 mM H_2O_2 or 100 ng/ml TNF-α. Cell viability was assessed by Trypan blue exclusion at 6 and 24 h, and representative results are shown in Fig. 3, *B* and *C*. The mean viability of untreated control cells at 6 and 24 h was reduced after infection with the pCLXSN retroviral vector (Fig. 3, *B* and *C*) compared with uninfected U937-ecoR cells (Fig. 1*A*). However, even in untreated cells, increased expres-

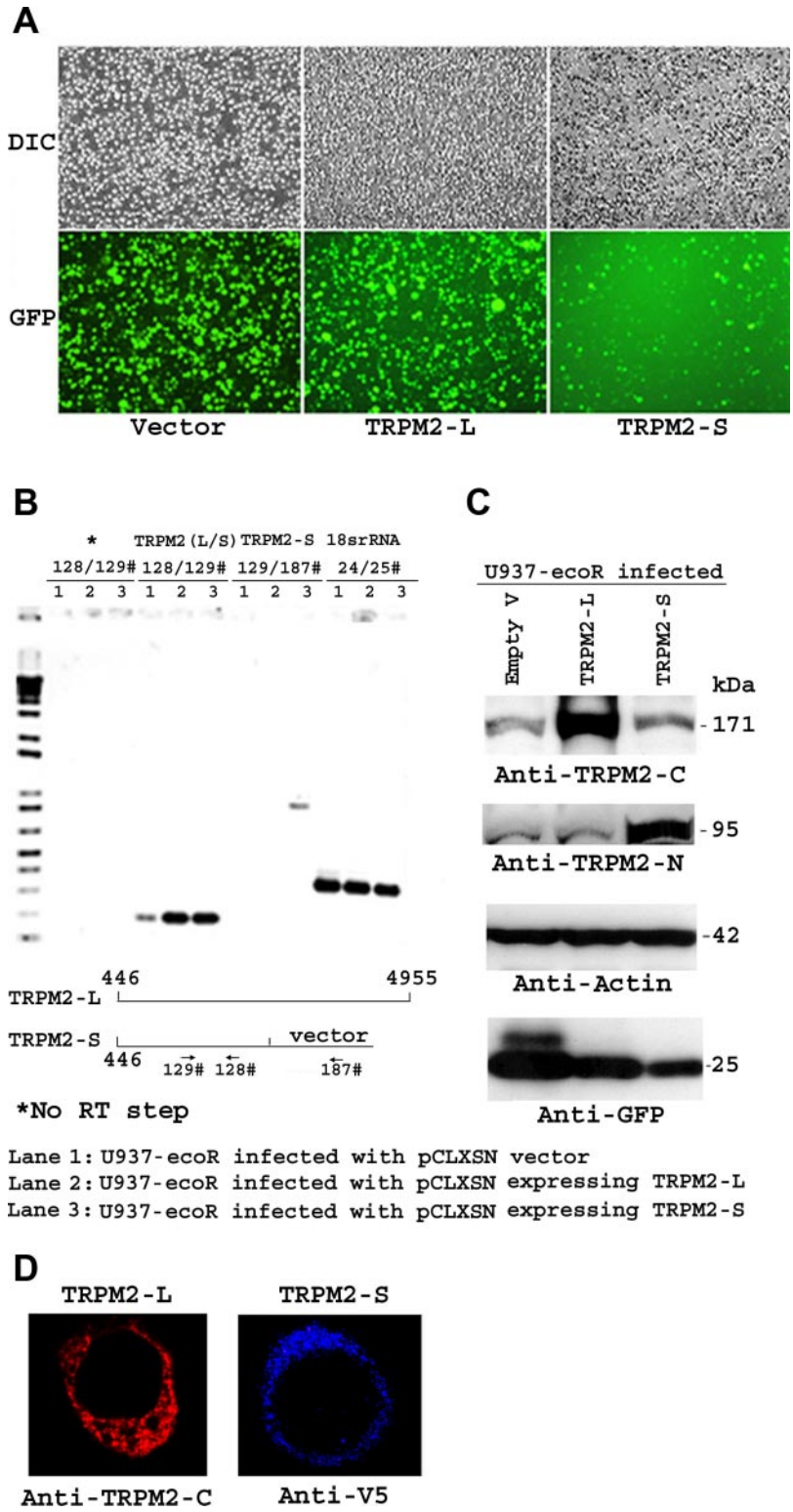

Fig. 2. Infection of U937-ecoR cells with pCLXSN-GFP expressing TRPM2 isoforms results in increased TRPM2 expression. *A*: green fluorescent protein (GFP) fluorescence was detected in the majority of U937-ecoR cells infected with pCLXSN empty vector or pCLXSN expressing TRPM2-L or TRPM2-S, confirming high infection efficiency. These results are representative of GFP fluorescence, which was examined with every experiment performed with retrovirus-infected cells. DIC, differential interference contrast. *B*: RT-PCR was performed with RNA isolated from U937-ecoR cells infected with empty pCLXSN vector (*lane 1*), pCLXSN expressing TRPM2-L (*lane 2*), or pCLXSN expressing TRPM2-S (*lane 3*). No PCR bands were observed without the RT step (*panel 1*). Primers specific for TRPM2 (L/S) (128, 129) detected all TRPM2 isoforms (*panel 2*). Primers 129 and 187 were specific for TRPM2-S expressed from the retroviral vector (*panel 3*). RT-PCR with primers for 18S rRNA confirmed the quality of RNA preparation (*panel 4*). This experiment was performed twice with similar results. *C*: Western blot analysis was performed with lysates from U937-ecoR cells infected with pCLXSN empty vector or pCLXSN expressing TRPM2-L or TRPM2-S. Immunoblotting with anti-TRPM2-C and anti-TRPM2-N antibodies confirmed increased expression of TRPM2-L and TRPM2-S, respectively, from their appropriate vectors. Immunoblotting with anti-actin antibody confirmed equivalent loading of lanes. Anti-GFP antibody confirmed GFP expression. Similar results were obtained with Western blot analysis of U937-ecoR cells after 4 separate infections. *D*: U937-ecoR cells infected with pCLXSN vector expressing TRPM2-L were stained with anti-TRPM2-C antibody and donkey anti-rabbit rhodamine red. U937-ecoR cells infected with pCLXSN vector expressing TRPM2-S were stained with anti-V5 antibody and donkey anti-mouse Cy5, followed by confocal microscopy. Representative results are shown.

sion of TRPM2-L resulted in significantly reduced cell viability ($P < 0.02$). At 6 h after treatment with 1 mM H_2O_2 or 100 ng/ml TNF-α, cells expressing TRPM2-L had cell viability reduced to 24 ± 1% and 46 ± 2%, respectively, a significant reduction compared with cells infected with vector alone ($P < 0.02$) or TRPM2-S ($P < 0.001$) (Fig. 3*B*). At 24 h, there was a further decrease in cell viability to 11 ± 1% after treatment with H_2O_2 ($P < 0.001$) and to 27 ± 1% after treatment with TNF-α ($P < 0.02$) (Fig. 3*C*). Similar results were observed in three experiments, confirming the involvement of TRPM2-L in mediating cell death in response to oxidative stress or TNF-α. In contrast, cells expressing TRPM2-S had significantly higher viability after treatment with H_2O_2 or TNF-α than either cells expressing vector alone ($P < 0.05$) or cells expressing in-

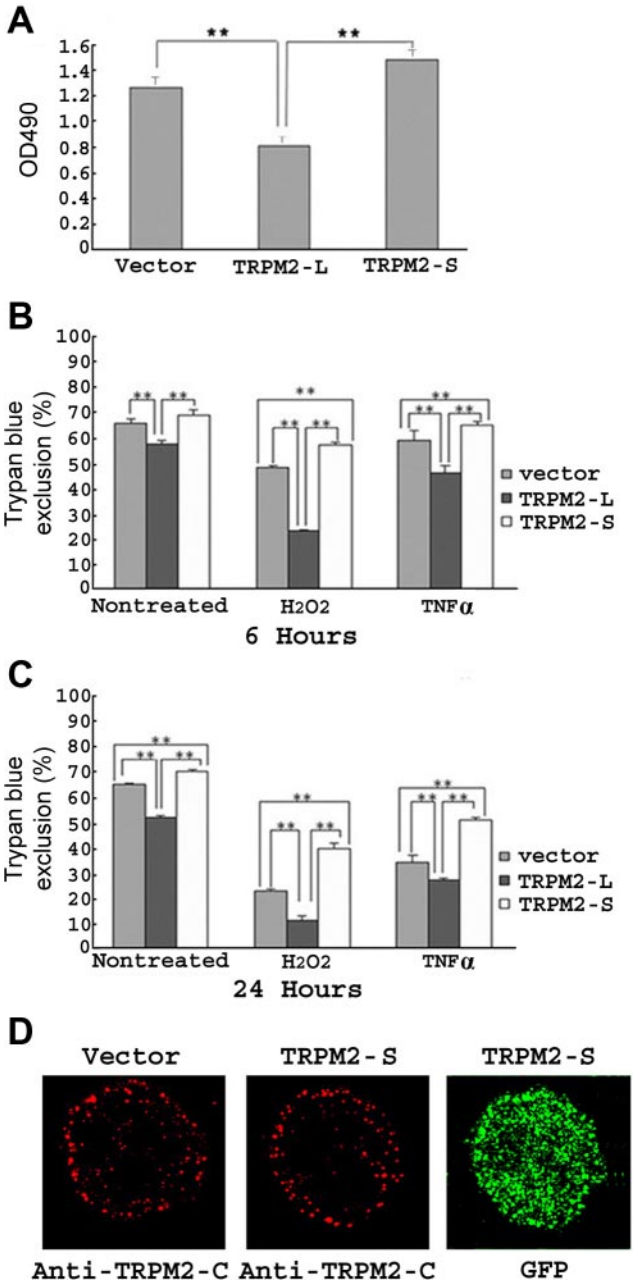

Fig. 3. Influence of TRPM2-L and TRPM2-S isoforms on U937-ecoR proliferation and viability. *A*: U937-ecoR cells were infected with empty pCLXSN vector or pCLXSN expressing TRPM2-L or TRPM2-S. Cell proliferation was measured with the CellTiter 96 Aq_{ueous} One Solution cell proliferation assay. Proliferation was significantly reduced in cells expressing increased TRPM2-L compared with cells expressing increased TRPM2-S or cells infected with empty vector. Representative results of 3 experiments are shown. OD_{490}, optical density at 490 nm. *B*: U937-ecoR cells infected with empty pCLXSN vector (vector) or pCLXSN expressing TRPM2-L or TRPM2-S were treated with 0 or 1 mM H_2O_2 or 100 ng/ml TNF-α for 6 h. Cells expressing TRPM2-L demonstrated significantly reduced cell viability ($P < 0.02$), whereas cells expressing increased TRPM2-S demonstrated significantly enhanced cell viability ($P < 0.05$). *C*: U937-ecoR cells described in *B* were treated with 0 or 1 mM H_2O_2 or 100 ng/ml TNF-α for 24 h. Cells expressing TRPM2-L demonstrated significantly reduced cell viability ($P < 0.02$), whereas cells expressing increased TRPM2-S demonstrated significantly enhanced cell viability ($P < 0.001$). Experiments in *B* and *C* were repeated 3 times with similar results. **Significant differences between groups ($P < 0.05$). *D*: U937-ecoR cells infected with pCLXSN empty vector or vector expressing TRPM2-S were stained with anti-TRPM2-C antibody and donkey anti-rabbit rhodamine red to detect endogenous TRPM2-L. Representative results after confocal microscopy are shown. GFP fluorescence in cells expressing TRPM2-S from pCLXSN is demonstrated.

creased levels of TRPM2-L ($P < 0.001$) (Fig. 3, *B* and *C*). These data demonstrate that TRPM2-S is able to inhibit cell death in response to TNF-α as well H_2O_2 (47). We previously determined (47) that although TRPM2-S directly interacts with TRPM2-L, TRPM2-S does not change the intracellular localization of TRPM2-L. Here we performed immunofluorescence to examine the intracellular localization of endogenous TRPM2-L in cells infected with empty pCLXSN-GFP vector or pCLXSN expressing TRPM2-S (Fig. 3*D*). GFP fluorescence identified successfully infected cells, but Alexa Fluor 488 could not be used as the secondary antibody because its excitation and emission wavelengths overlap with those of GFP. Endogenous TRPM2-L detection was less intense when anti-rabbit rhodamine red was used as the secondary antibody. However, no change in the intracellular localization of endogenous TRPM2-L was observed in U937-ecoR cells expressing retroviral TRPM2-S compared with empty vector.

To examine the role of TRPM2 in induction of apoptosis in response to oxidative stress or TNF-α, U937-ecoR cells expressing increased levels of TRPM2-L or TRPM2-S were treated with 0 or 1 mM H_2O_2 or 100 ng/ml TNF-α. Apoptosis was assessed at 6 h after treatment by labeling cells with Alexa Fluor 594 annexin V conjugates; annexin V binds to phosphatidylserine on the surface of early apoptotic cells. A visual representation of results is shown in Fig. 4*A*. Treatment of cells expressing increased levels of TRPM2-L with H_2O_2 resulted in a higher percentage of early apoptotic cells (41%, 108 cells counted) compared with cells infected with vector alone (25%, 97 cell counted). Cells expressing increased TRPM2-S demonstrated barely detectable apoptosis (13%, 145 cells counted). Results were similar after treatment with TNF-α (not shown). Viability of U937-ecoR cells was also measured 6 h after treatment with 1 mM H_2O_2 by staining with annexin V-PE and 7-AAD, followed by flow cytometry (Fig. 4*B*). In Fig. 4*B*, *top*, representative flow analysis of dead cells stained with 7-AAD (*top*) or apoptotic cells stained with Annexin V-PE (*right*) is shown; in three experiments, viable cells (*bottom left* corner) represented 62 ± 1% of cells infected with empty vector, 40 ± 1% of cells infected with vector expressing TRPM2-L, and 70 ± 1% of cells infected with vector expressing TRPM2-S. Figure 4*B*, *bottom*, shows a representative profile of 2×10^5 cells stained with annexin V-PE. In these three experiments, positive staining was detected in 37 ± 1% of cells infected with empty vector, 57 ± 1% of cells infected with vector expressing TRPM2-L, and 29 ± 1% of cells infected with vector expressing TRPM2-S. The viability of cells expressing TRPM2-L was significantly lower ($P < 0.001$) and the number of apoptotic cells was significantly higher ($P < 0.001$) compared with cells expressing empty vector or TRPM2-S. In contrast, the viability of cells expressing TRPM2-S was significantly higher ($P < 0.001$) than cells expressing vector alone. Three separate experiments performed in triplicate showed similar results. These results confirm that TRPM2-L enhanced cell death after oxidative stress or TNF-α treatment, whereas expression of TRPM2-S preserved cell viability.

TRPM2-S inhibits calcium influx in U937 cells in response to oxidative stress or TNF-α. We established a system to examine regulation of calcium influx through individual TRPC in single cells (7, 8, 47). U937-ecoR cells were infected with empty pCLXSN retroviral vector or pCLXSN expressing TRPM2-L or TRPM2-S. Successful infection of individual

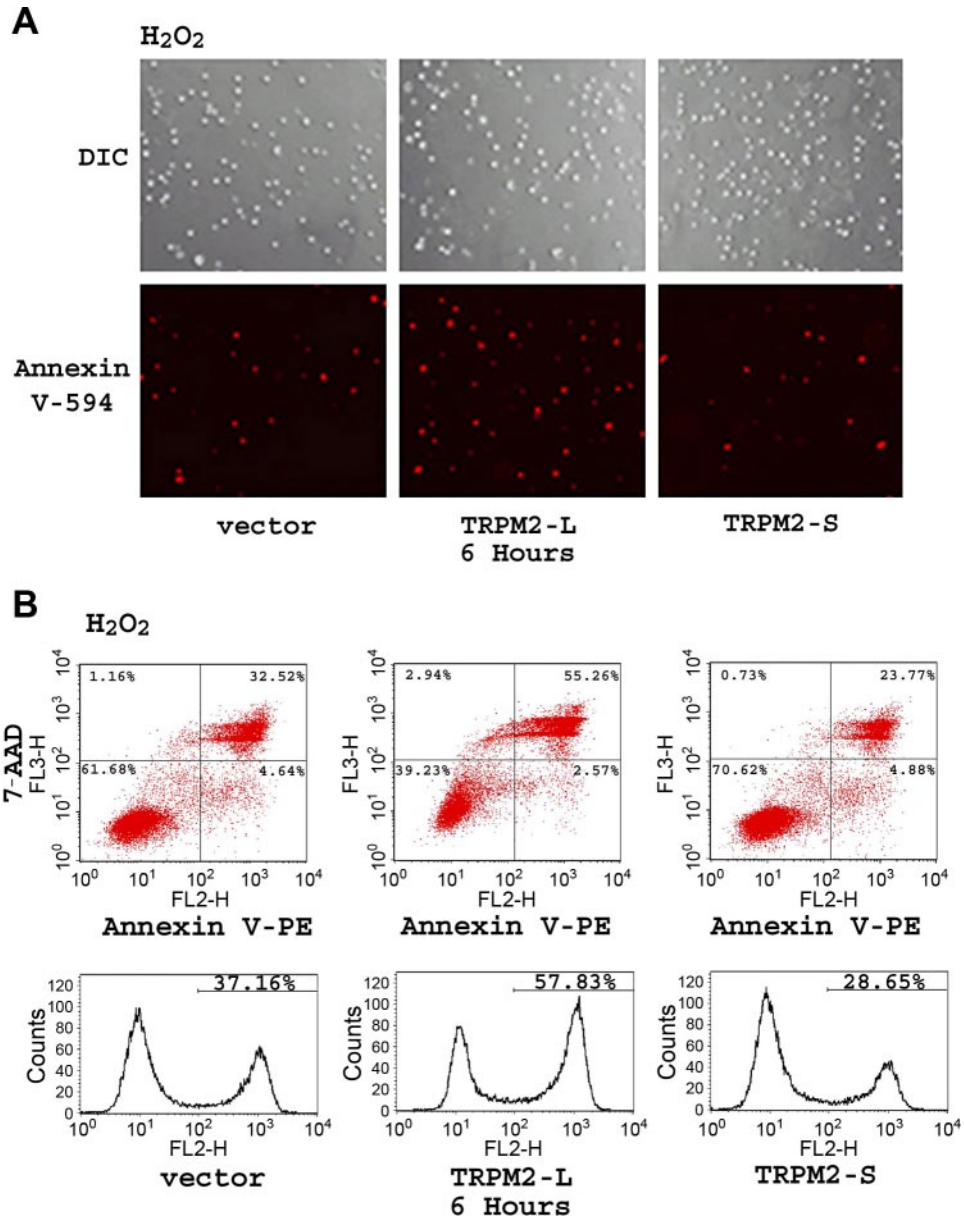

Fig. 4. Influence of TRPM2-L and TRPM2-S isoforms on induction of apoptosis. U937-ecoR cells infected with empty pCLXSN vector or pCLXSN vector expressing TRPM2-L or TRPM2-S were treated with 1 mM H_2O_2 for 6 h. *A*: the number of apoptotic cells was assessed by Alexa Fluor 594 annexin V staining. Representative results of 4 experiments are shown. *B*: the viability of U937-ecoR cells was measured by staining with annexin V-PE and 7-aminoactinomycin (7-AAD), followed by flow cytometry. *Top*: the *x*-axis indicates the intensity of annexin V-PE staining (FL2-H) and the *y*-axis that of 7-AAD (FL3-H). Viable cells at *bottom left* are annexin V-PE$^-$ and 7-AAD$^-$; early apoptotic cells at *bottom right* are annexin V-PE$^+$ and 7-AAD$^-$; cells in late apoptosis or dead at *top right* are annexin V-PE$^+$ and 7-AAD$^+$; and dead cells at *top left* are annexin V-PE$^-$ and 7-AAD$^+$. *Bottom*: a representative profile of 2×10^5 cells stained with annexin V-PE. Representative profiles of 3 similar experiments performed in triplicate are shown.

cells was confirmed by detection of GFP with our digital video imaging system. The Fura red fluorescence intensity ratio (F_{440}/F_{490}) was measured in single cells with digital video imaging at baseline and at intervals over 20 min after exposure to 1 mM H_2O_2 or 100 ng/ml TNF-α, and $[Ca^{2+}]_i$ was calculated. Cells infected with empty vector and treated with H_2O_2 demonstrated an increase in $[Ca^{2+}]_i$ from 39 ± 2 to 122 ± 5 nM, 238 ± 21% above baseline (Table 1). The increase in $[Ca^{2+}]_i$ in response to H_2O_2 was significantly greater in cells overexpressing TRPM2-L and significantly lower in cells overexpressing TRPM2-S (Table 1). Results were similar after treatment of U937-ecoR cells with TNF-α. These data demonstrate the importance of TRPM2 in regulation of $[Ca^{2+}]_i$ in response to oxidative stress or after exposure to TNF-α and confirm the ability of the physiological isoform TRPM2-S to inhibit the rise in $[Ca^{2+}]_i$.

Although TRPM2 channel activity has been characterized (18, 24, 36, 43), we performed experiments to confirm that the

Table 1. *Influence of TRPM2 isoforms on Ca^{2+} influx stimulated by H_2O_2 or TNF-α*

			$[Ca^{2+}]_i$, nM		
pCLXSN	*n*	Stimulation	Baseline	Peak	%Inc
Vector	36	H_2O_2	39±2	122±5	238±21
TRPM2-L	31	H_2O_2	37±2	213±28	554±94*
TRPM2-S	36	H_2O_2	42±2	84±4	108±10*
Vector	37	TNF-α	39±2	105±4	184±13
TRPM2-L	28	TNFα	38±3	134±4	309±27*
TRPM2-S	34	TNF-α	39±2	84±4	125±9*

Intracellular Ca^{2+} concentration ($[Ca^{2+}]_i$) values are means ± SE for *n* cells studied in 6 experiments. U937-ecoR cells were infected with pCLXSN empty vector or pCLXSN expressing TRPM2-L or TRPM2-S. At 3–5 days after infection, cells were loaded with Fura red. $[Ca^{2+}]_i$ was measured in single cells at baseline and by monitoring over 20 min after stimulation with 1 mM H_2O_2 or 100 ng/ml TNF-α. %Increase above baseline (%Inc) = (peak $[Ca^{2+}]_i$/baseline $[Ca^{2+}]_i$) × 100 − 100 (baseline). *Significant difference from cells transfected with empty vector ($P \leq 0.001$).

$[Ca^{2+}]_i$ increase in response to H_2O_2 or TNF-α in U937-ecoR cells originated from external Ca^{2+} influx rather than internal store release. U937-ecoR cells infected with pCLXSN vector expressing TRPM2-L were loaded with Fura red and treated with H_2O_2 or TNF-α in the presence of Ca^{2+} (0.68 mM) or in its absence (2 mM EGTA). $[Ca^{2+}]_i$ was measured at 5-s intervals for the first 30 s and at 15-s intervals for the next 90 s. Representative results of changes in single cells are shown in Fig. 5. No significant change in $[Ca^{2+}]_i$ was observed after H_2O_2 or TNF-α treatment in the absence of extracellular Ca^{2+}. In addition, no significant increase in $[Ca^{2+}]_i$ was observed in the first 2 min after treatment with H_2O_2 or TNF-α, as would have been expected after intracellular Ca^{2+} release. These data suggest that the major component of the H_2O_2- or TNF-α-stimulated rise in $[Ca^{2+}]_i$ in TRPM2-expressing cells is extracellular Ca^{2+} influx.

TRPM2 activation results in caspase-8, -9, -3, and -7 and PARP cleavage. The mechanism of induction of cell death after TRPM2 activation was examined with U937-ecoR cells infected with pCLXSN empty vector or pCLXSN expressing TRPM2-L or TRPM2-S. Cell lysates were prepared from cells that were untreated or treated for 6 h with H_2O_2, and immunoblotting was performed with antibodies to caspases-8, -9, -3, and -7, PARP, and Bcl-2. Treatment with H_2O_2 resulted in cleavage of procaspases-8, -9, -3, and -7, which was much greater in cells overexpressing TRPM2-L (Fig. 6). These experiments demonstrate that both extrinsic and intrinsic death pathways are involved in TRPM2-mediated apoptosis, leading to activation of caspases-3 and -7 (33). Caspase cleavage of the 116-kDa PARP protein to an 89-kDa polypeptide is an indicator of cells undergoing apoptosis. Enhanced cleavage of PARP was observed in cells overexpressing TRPM2-L and decreased cleavage in cells overexpressing TRPM2-S. Bcl-2 levels were unchanged and confirmed equal loading of total protein in each lane of the Western blots.

We then examined the role of $[Ca^{2+}]_i$ in mediating cell death through TRPM2. U937-ecoR cells were loaded with the intracellular Ca^{2+} chelator BAPTA-AM before treatment with H_2O_2, and $[Ca^{2+}]_i$ was measured over 20 min with digital video imaging. The increase in $[Ca^{2+}]_i$ observed after treat-

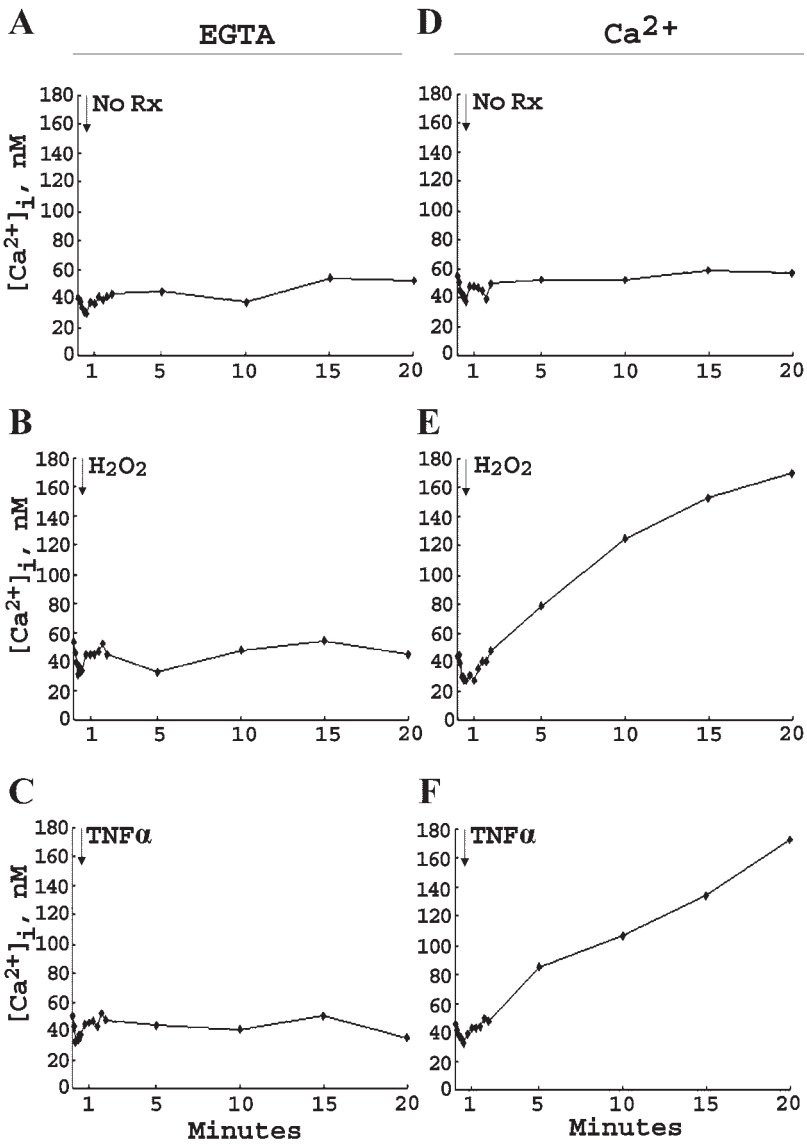

Fig. 5. Time course of intracellular Ca^{2+} concentration ($[Ca^{2+}]_i$) after H_2O_2 or TNF-α treatment. Fura red-loaded U937-ecoR cells infected with pCLXSN expressing TRPM2-L were treated at 0 min with vehicle (no R_x; *A*, *D*), 1 mM H_2O_2 (*B*, *E*), or 100 ng/ml TNF-α (*C*, *F*) in the absence (2 mM EGTA) or presence (0.68 mM) of calcium. $[Ca^{2+}]_i$ was measured in representative cells at baseline, at 5-s intervals for the first 30 s, at 15-s intervals for the next 90 s, and then at 5-min intervals to 20 min. Five experiments were performed, and 8–43 cells were studied in each group with similar results.

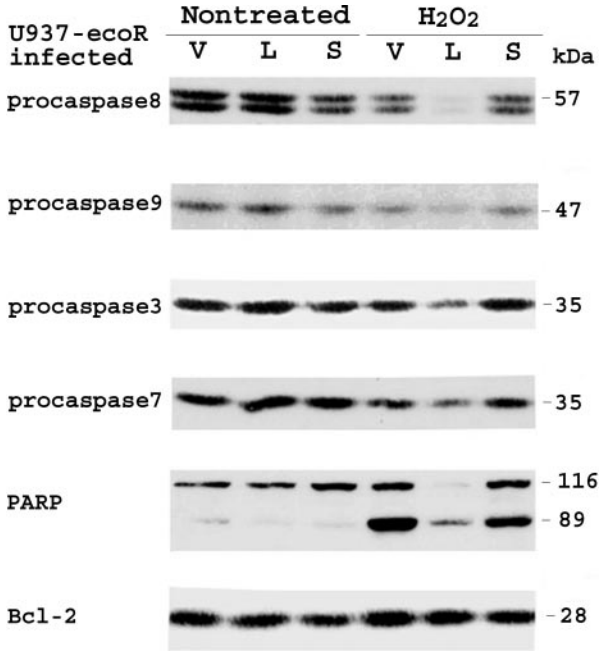

Fig. 6. Involvement of caspases-8, -9, -3, and -7 and poly(ADP-ribose)polymerase (PARP) in TRPM2-mediated cell death. Western blot analysis was performed on lysates from U937-ecoR cells infected with pCLXSN empty vector (V) or pCLXSN expressing TRPM2-L (L) or TRPM2-S (S), untreated or treated for 6 h with 1 mM H_2O_2. Blots were probed with anti-caspase-8, anti-caspase-9, anti-caspase-3, anti-caspase-7, anti-PARP, and anti-Bcl-2 antibodies, followed by the appropriate horseradish peroxidase (HRP)-conjugated antibodies and enhanced chemiluminescence (ECL). This experiment was performed twice with identical results.

ment with H_2O_2 was significantly inhibited by 10 μM BAPTA-AM, demonstrating that the majority of entering Ca^{2+} was buffered (Fig. 7*A*). Results were similar when cells were exposed to 20 μM BAPTA-AM (not shown). To determine whether cell death mediated by H_2O_2 requires an increase in $[Ca^{2+}]_i$, U937-ecoR cells infected with empty pCLXSN retroviral vector or pCLXSN expressing TRPM2-L were treated with H_2O_2 alone or H_2O_2 with BAPTA-AM. Viability of cells incubated with 1 mM H_2O_2 for 6 h was 59 ± 1% for vector-infected U937-ecoR cells and 14 ± 2% for TRPM2-expressing cells (Fig. 7*B*). In contrast, the viabilities of cells incubated with 1 mM H_2O_2 and 10 μM BAPTA-AM were 82 ± 1% and 53 ± 1% for vector-infected and TRPM2-expressing cells, respectively. Buffering of the rise in $[Ca^{2+}]_i$ with BAPTA-AM in TRPM2-expressing cells inhibited H_2O_2-induced cleavage of procaspases-8, -9, -3, and -7 and reduced inactivation of PARP (Fig. 7*C*). These data demonstrate the critical role of the increase in $[Ca^{2+}]_i$ in induction of hematopoietic cell death by H_2O_2 through TRPM2.

Downregulation of endogenous TRPM2 with RNAi. To examine the role of endogenous TRPM2 in H_2O_2- or TNF-α-mediated cell death, three siRNA oligonucleotides were designed that were targeted to the 5′ coding region of TRPM2. The effectiveness of siRNA in reducing TRPM2 expression was first characterized in 293T cells. 293T cells were cotransfected with the pSuper vector expressing siRNA oligonucleotides targeted to TRPM2 and with TRPM2-L in pcDNA3. Western blotting with anti-TRPM2-C antibody (47) revealed suppression of heterologous TRPM2 protein expression with all three siRNA directed to TRPM2 (Fig. 8*A*). Nearly complete suppression was observed with siRNA3. None of the three siRNA targeted to TRPM2 had an effect on actin expression. To confirm the specificity of the siRNA oligonucleotides for TRPM2, 293T cells were transfected with TRPC6 in pcDNA3 (8) and with pSuper vector expressing siRNA3 directed to TRPM2. No inhibition of TRPC6 expression was observed, further demonstrating the specificity of siRNA reagents targeted to TRPM2 (Fig. 8*A*).

To examine the functional consequences of RNAi-induced depletion of TRPM2 on cell viability, U937-ecoR cells were infected with pSuppressorRetro Vector expressing siRNA targeted to TRPM2 (siRNA3) or to luciferase or with empty vector. RT-PCR performed with primers directed to TRPM2 demonstrated that endogenous TRPM2 RNA was successfully downregulated by siRNA3. In contrast, TRPM2 RNA levels were unchanged in cells infected with empty vector or with retrovirus expressing siRNA directed to luciferase (Fig. 8*B*, *left*). RT-PCR with primers to the neomycin resistance gene present in the retroviral vector demonstrated that all groups of U937-ecoR cells were successfully infected with pSuppressorRetro (Fig. 8*B*, *center*, *lanes 2–4*). The quality of the RNA preparations was confirmed by RT-PCR with primers directed to 18S rRNA (Fig. 8*B*, *right*). Western blot analysis (Fig. 8*C*) and immunofluorescence (Fig. 8*D*) demonstrated the ability of RNAi targeted to TRPM2 to reduce endogenous TRPM2 protein levels, which was not observed in cells expressing empty vector or TRPM2 targeted to luciferase. These studies also showed that RNAi directed to the TRPM2 significantly reduced endogenous TRPM2 protein expression in the majority of cells. To examine the functional role of endogenous TRPM2 in hematopoietic cell survival, U937-ecoR cells infected with pSuppressorRetro Vector expressing siRNAs directed to TRPM2 or to luciferase were treated with 0 or 1 mM H_2O_2 or 100 ng/ml TNF-α. Reduction of TRPM2 expression resulted in significant enhancement of cell viability at 24 h after treatment with H_2O_2 ($P < 0.001$) or TNF-α ($P < 0.05$) (Fig. 9*A*), compared with cells expressing siRNA directed to luciferase or empty vector.

To examine the functional consequences of RNAi-induced suppression of TRPM2 on induction of apoptosis after oxidative stress, U937-ecoR cells infected with retrovirus expressing siRNAs targeted to TRPM2 or to luciferase were treated with 1 mM H_2O_2 or 100 ng/ml TNF-α for 24 h. Apoptosis was assessed by labeling of cells with Alexa Fluor 488 annexin V conjugates. Representative results are shown in Fig. 9*B*. Downregulation of endogenous TRPM2 resulted in reduced numbers of apoptotic cells (8%, 221 cells counted) compared with cells infected with empty vector (15%, 307 cells counted) or with vector expressing siRNA targeted to luciferase (18%, 283 cells counted) after H_2O_2 treatment. Similarly, downregulation of endogenous TRPM2 resulted in a reduced number of apoptotic cells (19%, 131 cells counted) after treatment with 100 ng/ml TNF-α for 24 h (Fig. 9*B*) compared with cells infected with empty vector (25%, 210 cells counted) or cells expressing siRNA targeted to luciferase (33%, 285 cells counted). Viability of U937-ecoR cells after downmodulation of endogenous TRPM2 was also measured 24 h after treatment with 1 mM H_2O_2 by staining with annexin V-PE and 7-AAD followed by flow cytometry (Fig. 9*C*). In Fig. 9*C*, *top*, representative flow analysis of dead cells stained with 7-AAD or apoptotic cells stained with Annexin V-PE is shown; in three experiments,

viable cells represented 39 ± 1% of cells infected with empty vector, 57 ± 1% of cells infected with vector expressing RNAi targeted to TRPM2, and 40 ± 1% of cells infected with RNAi targeted to luciferase. Figure 9*C*, *bottom*, shows a representative profile of 2×10^5 cells stained with annexin V-PE; in three experiments, positive staining with annexin V-PE was detected in 57 ± 1% of cells infected with empty vector, 41 ± 1% of cells infected with vector targeted to TRPM2, and 57 ± 1% of cells infected with vector targeted to luciferase. The viability of cells in which TRPM2-L was downregulated was significantly higher ($P < 0.001$) and the number of apoptotic cells was significantly lower ($P < 0.001$) compared with cells expressing empty vector or RNAi targeted to luciferase. Triplicates of this experiment showed similar results.

We examined the effects of downregulation of TRPM2 on PARP cleavage, an end point of caspase activation, after treatment with 1 mM H_2O_2 for 24 h (Fig. 9*D*). After treatment with H_2O_2, much less cleavage of PARP was observed in cells in which endogenous TRPM2 had been reduced, consistent with our observations on cell viability. These results demonstrate the important role of endogenous TRPM2 in the susceptibility of hematopoietic cells to death after oxidative stress and in response to TNF-α.

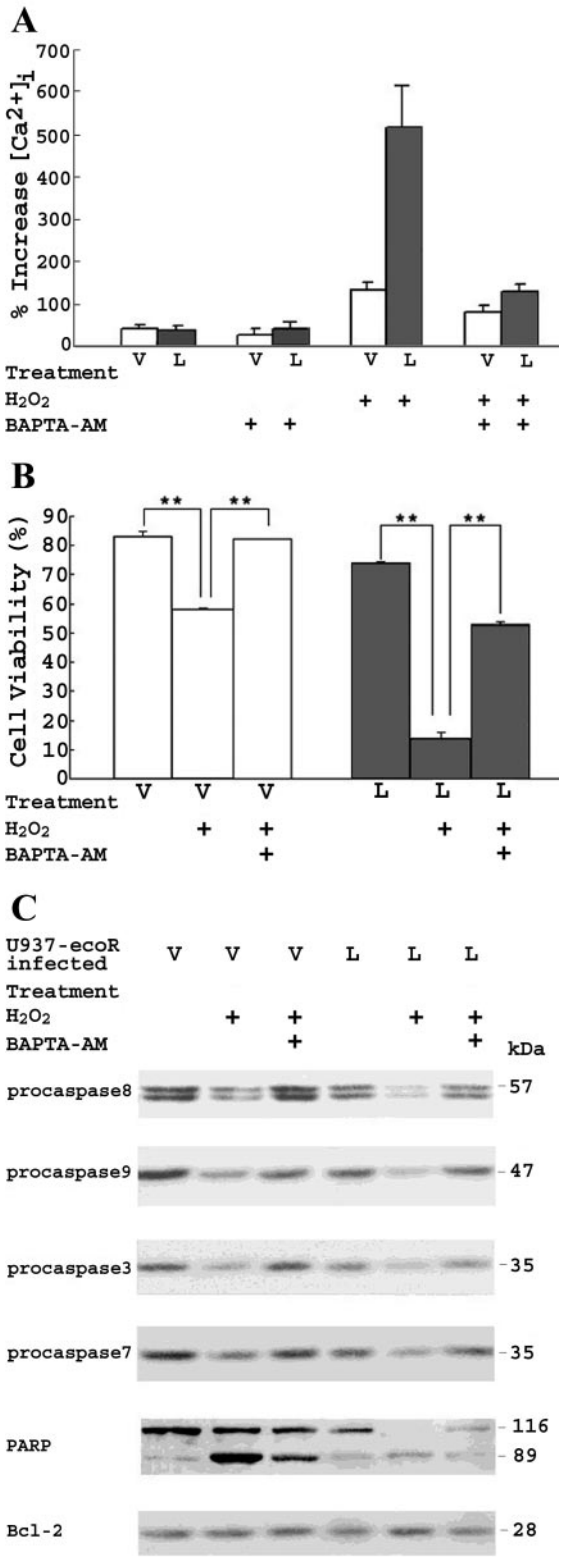

DISCUSSION

In this study, we examined the function of the cation-permeable channel TRPM2 and the mechanism through which its activation contributes to induction of cell death. Overexpression of TRPM2 in human monocytic U937 cells with retroviral infection resulted in significant increase in $[Ca^{2+}]_i$, decrease in cell viability, and increase in apoptosis after exposure to H_2O_2 or TNF-α. In contrast, inhibition of TRPM2 function by depletion of endogenous TRPM2 by RNAi, blockade of the increase in $[Ca^{2+}]_i$ through TRPM2 by Ca^{2+} chelation, or expression of the dominant-negative TRPM2-S splice variant significantly protected cell viability after exposure to oxidative stress or TNF-α. This work emphasizes the important role of the ion channel TRPM2 in oxidative stress- and TNF-α-induced cell death by multiple approaches.

Intracellular calcium is an universally important second messenger that influences many cell functions (5). Calcium signals in cells are finely tuned, and $[Ca^{2+}]_i$ provides an important regulatory role, both in cell survival and proliferation and in apoptotic or necrotic cell death (33). Recent work in hematopoietic cells suggests that the opposing effects of $[Ca^{2+}]_i$ on cell survival depend on the duration and amplitude of the calcium signal (3, 4). Transient elevation of $[Ca^{2+}]_i$ resulted in transient activation of ERK1/2 and upregulation of Bcl-2, protecting cells from apoptosis. In contrast, high and sustained increases in $[Ca^{2+}]_i$ resulted in sustained activation of ERK1/2 and apoptosis. Our data demonstrate that TRPM2

Fig. 7. TRPM2-mediated cell death and caspase/PARP cleavage require calcium influx. *A*: U937-ecoR cells infected with pCLXSN empty vector or pCLXSN expressing TRPM2-L were treated with 0 or 1 mM H_2O_2 for 20 min, with or without pretreatment for 60 min with 10 μM BAPTA-AM. $[Ca^{2+}]_i$ was measured at baseline and at 2- to 5-min intervals over 20 min. Mean ± SE % increase of peak $[Ca^{2+}]_i$ above baseline is shown. Sixteen to twenty-five cells were studied in each group in four experiments. *B*: cell viability was determined by Trypan blue exclusion after 6 h of treatment with 0 or 1 mM H_2O_2, with or without 10 μM BAPTA-AM. Mean ± SE numbers of viable cells are shown. **Significant difference ($P < 0.05$). Three experiments were performed with similar results. *C*: Western blot analysis was performed on lysates from U937-ecoR cells infected with pCLXSN empty vector or pCLXSN expressing TRPM2-L, treated for 6 h with 0 or 1 mM H_2O_2 with or without 10 μM BAPTA-AM. Blots were probed with anti-caspase-8, anti-caspase-9, anti-caspase-3, anti-caspase-7, anti-PARP, and anti-Bcl-2 antibodies followed by the appropriate HRP-conjugated antibodies and ECL.

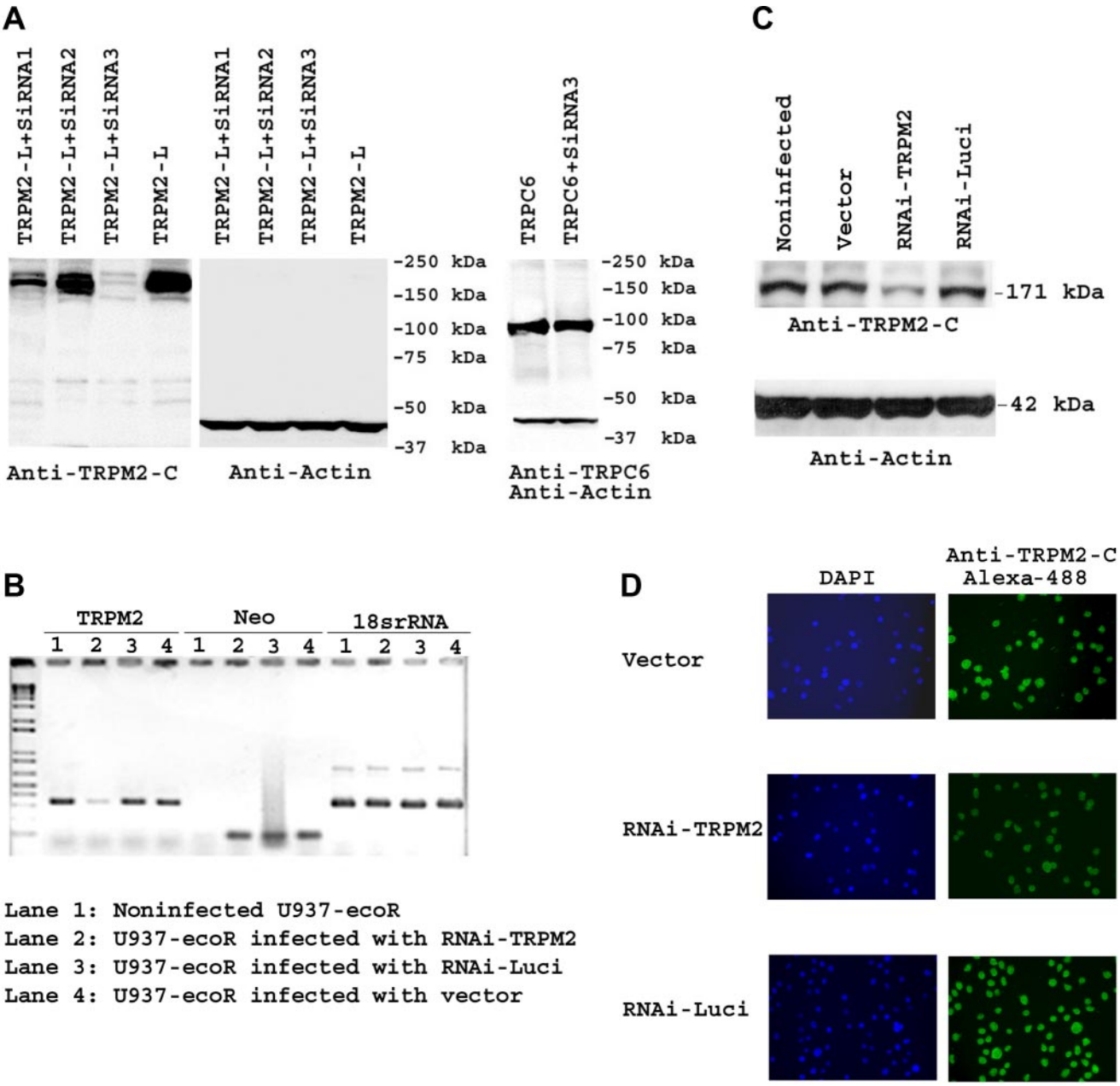

Fig. 8. Effectiveness of small interfering RNA (siRNA) in downregulation of TRPM2. *A*: 293T cells were transfected with TRPM2-L or TRPC-6 in pcDNA3, with or without pSuper vector expressing TRPM2 siRNA oligonucleotides. TRPM2 expression was measured by Western blotting with anti-TRPM2-C antibody and anti-rabbit-HRP-conjugated secondary antibody followed by ECL. Actin was assessed by staining with anti-actin antibody and TRPC6 with anti-TRPC6 antibody, followed by the same secondary. TRPC6 blots were probed simultaneously with anti-TRPC6 and anti-actin antibodies. Experiments were performed twice with similar results. *B*: U937-ecoR cells were not infected (*lane 1*) or infected with pSuppressorRetro Vector expressing siRNA targeted to TRPM2 (*lane 2*), siRNA targeted to luciferase (*lane 3*), or empty vector (*lane 4*). RT-PCR with primers specific for TRPM2 demonstrated significant downregulation by siRNA targeted to TRPM2 (*left*). RT-PCR performed with primers for the retroviral neomycin gene (Neo) demonstrated high infection efficiency (*center*). RT-PCR with primers for 18S rRNA confirmed the quality of sample preparation (*right*). RT-PCR analysis was performed 4 times with identical results. *C*: Western blot of lysates from noninfected U937-ecoR cells or U937-ecoR cells expressing empty pSuppressorRetro vector or RNA interference (RNAi) targeted to TRPM2 or luciferase. Blots were probed with anti-TRPM2-C and secondary donkey anti-rabbit HRP antibodies to detect endogenous TRPM2 and anti-actin antibody to demonstrate equivalent loading of lanes. *D*: immunofluorescence of TRPM2 expression in U937-ecoR cells. Expression of endogenous TRPM2 was determined by staining cells with anti-TRPM2-C and goat anti-rabbit Alexa Fluor 488 antibodies. 4′,6-diamidino-2-phenylindole dihydrochloride (DAPI) was used to stain DNA. Fluorescence was detected with a Nikon TE2000 microscope.

activation by oxidant stress (H_2O_2) or TNF-α results in a sustained elevation in $[Ca^{2+}]_i$ (Fig. 5). Here we inhibited the increase in $[Ca^{2+}]_i$ with the Ca^{2+} chelator BAPTA, which blocks the elevation in $[Ca^{2+}]_i$ from both Ca^{2+} influx and internal Ca^{2+} release pathways. The effects of buffering the rise in $[Ca^{2+}]_i$ with BAPTA demonstrate one major finding of this work, that the mechanism of cell death after TRPM2 activation requires an increase in $[Ca^{2+}]_i$ and that viability of TRPM2-expressing cells is preserved when the increase in $[Ca^{2+}]_i$ is inhibited.

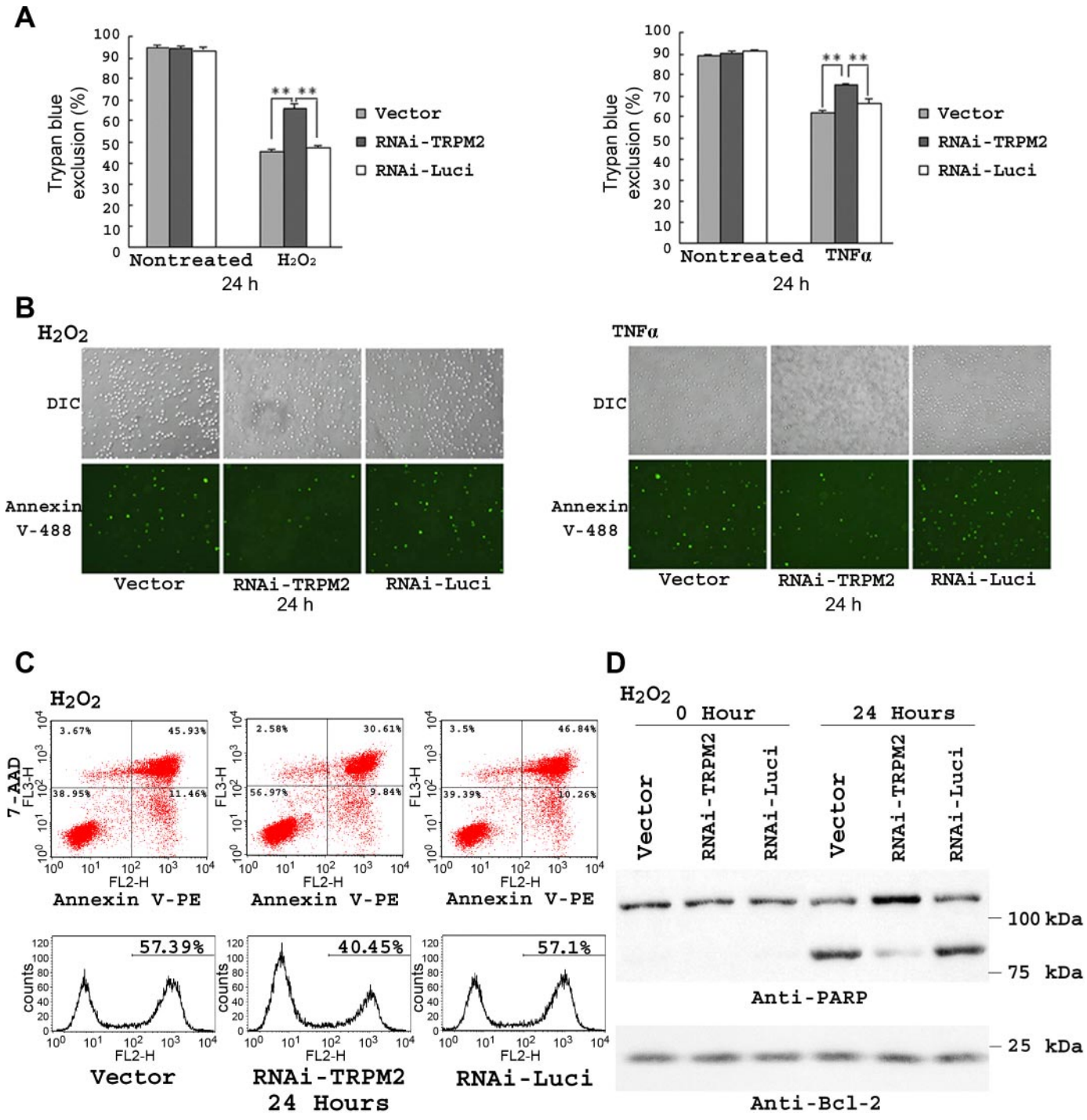

Fig. 9. Depletion of TRPM2 by RNAi suppresses cell death induced by H_2O_2 and TNF-α. U937-ecoR cells were infected with empty pSuppressorRetro vector or the same vector expressing siRNA targeted to TRPM2 or luciferase. Cells were treated with 0 or 1 mM H_2O_2 or 100 ng/ml TNF-α. *A*: cell viability was assessed by Trypan blue exclusion at 24 h. Compared with cells infected with empty vector (V) or siRNA directed to luciferase, downregulation of TRPM2 resulted in a significant increase in viability after treatment with H_2O_2 ($P < 0.001$) or TNF-α ($P < 0.001$). Representative results of 5 experiments performed with H_2O_2 and 3 experiments performed with TNF-α are shown. **Significant differences between groups; $P < 0.05$. *B*: U937-ecoR cells were infected as described in *A* and treated with 1 mM H_2O_2 or 100 ng/ml TNF-α for 24 h. Apoptotic cells were identified by staining with Alexa Fluor 488 annexin V conjugate. Two experiments with each factor were performed with similar results. *C*: the viability of U937-ecoR cells infected and treated as described in *A* and *B* was measured by staining with annexin V-PE and 7-AAD, followed by flow cytometry. *Top*: the *x*-axis indicates the intensity of annexin V-PE staining and the *y*-axis that of 7-AAD. *Bottom*: a representative profile of 2×10^5 cells stained with annexin V-PE is shown. *D*: Western blotting was performed on lysates from U937-ecoR cells before and after treatment with 1 mM H_2O_2 for 24 h. Blots were probed with anti-PARP antibody, followed by the appropriate HRP-conjugated antibodies and ECL. Blots were stripped and reprobed with anti-Bcl-2 antibody as a control.

The second major finding of this report is the delineation of a mechanism of cell death downstream of TRPM2 activation. Our data show that TRPM2 activation results in cleavage of procaspases-8, -9, -3, and -7 and PARP. These data demonstrate a signaling cascade downstream of TRPM2 leading to cell death, involving intrinsic (caspase-9) and extrinsic (caspase-8) cell death pathways and resulting in activation of the effector caspases -3 and -7. PARP is part of a protective mechanism involved in repair of DNA damage, and inactivation of PARP in TRPM2-expressing cells by PARP cleavage further contributes to apoptosis. Consistent with our observations, involvement of caspases-8 and -3 and PARP in H_2O_2-induced apoptosis has previously been reported (10, 22, 26, 48), but this is the first time this pathway has been linked to TRPM2 activation. Previously, Hara et al. (16) were unable to demonstrate a role for caspase-3 in H_2O_2-induced death in TRPM2-expressing HEK cells, possibly because of differences in the time course or concentration of H_2O_2 treatment or because of differences in cell type. Here inhibition of the rise in $[Ca^{2+}]_i$ with BAPTA blocked caspase and PARP cleavage in TRPM2-expressing cells, demonstrating that the rise in $[Ca^{2+}]_i$ precedes activation of the cascade. Few regulatory molecules have been identified that link elevation of $[Ca^{2+}]_i$ to caspase activation, and this area requires further investigation. However, apoptosis receptor with CARD (ARC), a member of the caspase recruitment domain (CARD) family, has been shown to interact with procaspase-8, and an elevation in $[Ca^{2+}]_i$ results in dissociation of ARC, leaving procaspase-8 susceptible to activation (21). In addition, elevation of $[Ca^{2+}]_i$ has been linked to mitochondrial cytochrome *c* release (15), which may result in caspase-9 activation. These are potential mechanisms through which an increase in $[Ca^{2+}]_i$ could activate both the intrinsic and extrinsic cell death pathways.

TRPM2 is activated by ADPR (16, 18, 35, 36, 39), and NAD and ADPR levels are increased by oxidative stress (36, 43). However, H_2O_2 has been reported to stimulate calcium influx through an alternative TRPM2 splice variant with a deletion in the COOH terminus, TRPM2-ΔC, whereas intracellular application of ADPR does not (43). This observation suggests that oxidative stress may also regulate TRPM2 through a mechanism independent of ADPR, a possibility that is unresolved (36). PARP inhibitors have recently been reported to suppress H_2O_2 activation of TRPM2, suggesting that TRPM2 activation by oxidative stress is dependent on PARP (13). These data combined with ours suggest a feedback loop: TRPM2 is activated by PARP, but TRPM2 activation in turn results in PARP cleavage and inactivation. This negative feedback may partially protect the cell from death, depending on the extent of activation of other pathways downstream of caspase-3. However, PARP inhibitors are not completely specific, and there is ambiguity about the role of PARP in TRPM2 activation (36). Further investigation is needed to delineate the pathways, particularly those involving ADPR and PARP, through which oxidative stress and TNF-α regulate TRPM2 channel opening.

Primary hematopoietic cells, including $CD34^+$ cells, erythroblasts derived from human erythroid progenitors (BFU-E), and human monocytes, express TRPM2 isoforms. A role in hematopoeisis has previously been demonstrated for three other ion channels: HERG potassium channels, which are involved in the proliferation of $CD34^+$ cells (37), a potassium inward rectifier (K_{ir}) current, which has a role in the early differentiation of $CD34^+$ cells (40), and TRPC2, which regulates calcium influx in response to erythropoietin stimulation (7, 8). TRPM2-like currents have been detected in primary granulocytes, and a role for TRPM2 in the oxidative burst following enhanced NAD and ADPR production and in chemoattraction of granulocytes has been proposed (18, 19). The studies presented here demonstrate that another function of TRPM2 expression in hematopoietic cells is regulation of $[Ca^{2+}]_i$, contributing to susceptibility to cell death under conditions of oxidative stress or increased TNF-α production.

Inhibition of endogenous TRPM2 channel function, by either downregulation with RNAi or expression of a dominant-negative splice variant (TRPM2-S), blocked calcium entry and protected cells from death after oxidative stress or exposure to TNF-α. Modulation of TRPM2 activity may have important therapeutic potential in a number of diseases. Inhibition of TRPM2 activity may protect the viability of cells after exposure to several toxic conditions, whereas enhancement of TRPM2 activity may have utility in increasing susceptibility of cells to death, for example, in treatment of malignancy. Our studies with TRPM2 are part of an increasing body of evidence characterizing ion channels expressed in nonexcitable cells (41). The expression of TRPM2 in many cell types including human brain, placenta, lung, and gastrointestinal tissues (16, 18, 39) suggests that studies delineating the function, regulation, and therapeutic manipulation of TRPM2 are likely to be relevant to many tissues.

GRANTS

This work was supported by grants from the National Institutes of Health (R01-DK-46778 and R01-HL-58672) and by a grant from the Four Diamonds Fund of The Pennsylvania State University College of Medicine.

REFERENCES

1. **Aarts M, Iihara K, Wei WL, Xiong ZG, Arundine M, Cerwinski W, MacDonald JF, and Tymianski M.** A key role for TRPM7 channels in anoxic neuronal death. *Cell* 115: 863–877, 2003.
2. **Alexander SP, Mathie A, and Peters JA.** Guide to receptors and channels, 1st edition. *Br J Pharmacol* 141, *Suppl* 1: S1–S126, 2004.
3. **Apati A, Janossy J, Brozik A, Bauer PI, and Magocsi M.** Calcium induces cell survival and proliferation through the activation of the MAPK pathway in a human hormone-dependent leukemia cell line, TF-1. *J Biol Chem* 278: 9235–9243, 2003.
4. **Apati A, Janossy J, Brozik A, and Magocsi M.** Effects of intracellular calcium on cell survival and the MAPK pathway in a human hormone-dependent leukemia cell line (TF-1). *Ann NY Acad Sci* 1010: 70–73, 2003.
5. **Berridge MJ, Lipp P, and Bootman MD.** The versatility and universality of calcium signalling. *Nat Rev Mol Cell Biol* 1: 11–21, 2000.
6. **Cheung JY, Zhang XQ, Bokvist K, Tillotson DL, and Miller BA.** Modulation of calcium channels in human erythroblasts by erythropoietin. *Blood* 89: 92–100, 1997.
7. **Chu X, Cheung JY, Barber DL, Birnbaumer L, Rothblum LI, Conrad K, Abrasonis V, Chan YM, Stahl R, Carey DJ, and Miller BA.** Erythropoietin modulates calcium influx through TRPC2. *J Biol Chem* 277: 34375–34382, 2002.
8. **Chu X, Tong Q, Cheung JY, Wozney J, Conrad K, Mazack V, Zhang W, Stahl R, Barber DL, and Miller BA.** Interaction of TRPC2 and TRPC6 in erythropoietin modulation of calcium influx. *J Biol Chem* 279: 10514–10522, 2004.
9. **Clapham DE.** TRP channels as cellular sensors. *Nature* 426: 517–524, 2003.
10. **Denning TL, Takaishi H, Crowe SE, Boldogh I, Jevnikar A, and Ernst PB.** Oxidative stress induces the expression of Fas and Fas ligand and apoptosis in murine intestinal epithelial cells. *Free Radic Biol Med* 33: 1641–1650, 2002.
11. **Duncan LM, Deeds J, Hunter J, Shao J, Holmgren LM, Woolf EA, Tepper RI, and Shyjan AW.** Down-regulation of the novel gene melasta-

tin correlates with potential for melanoma metastasis. *Cancer Res* 58: 1515–1520, 1998.
12. **Elbashir SM, Harborth J, Lendeckel W, Yalcin A, Weber K, and Tuschl T.** Duplexes of 21-nucleotide RNAs mediate RNA interference in cultured mammalian cells. *Nature* 411: 494–498, 2001.
13. **Fonfria E, Marshall ICB, Benham CD, Boyfield I, Brown JD, Hill K, Hughes JP, Skaper SD, Scharenberg AM, and McNulty S.** TRPM2 channel opening in response to oxidative stress is dependent on activation of poly(ADP-ribose) polymerase. *Br J Pharmacol* 143: 186–192, 2004.
14. **Garland D and Russell P.** Phosphorylation of lens fiber cell membrane proteins. *Proc Natl Acad Sci USA* 82: 653–657, 1985.
15. **Gogvadze V, Robertson JD, Zhivotovsky B, and Orrenius S.** Cytochrome *c* release occurs via Ca^{2+}-dependent and Ca^{2+}-independent mechanisms that are regulated by Bax. *J Biol Chem* 276: 19066–19071, 2001.
16. **Hara Y, Wakamori M, Ishii M, Maeno E, Nishida M, Yoshida T, Yamada H, Shimizu S, Mori E, Kudoh J, Shimizu N, Kurose H, Okada Y, Imoto K, and Mori Y.** LTRPC2 Ca^{2+}-permeable channel activated by changes in redox status confers susceptibility to cell death. *Mol Cell* 9: 163–173, 2002.
17. **Harteneck C, Plant TD, and Schultz G.** From worm to man: three subfamilies of TRP channels. *Trends Neurosci* 23: 159–166, 2000.
18. **Heiner I, Eisfeld J, Halaszovich CR, Wehage E, Jungling E, Zitt C, and Luckhoff A.** Expression profile of the transient receptor potential (TRP) family in neutrophil granulocytes: evidence for currents through long TRP channel 2 induced by ADP-ribose and NAD. *Biochem J* 371: 1045–1053, 2003.
19. **Heiner I, Eisfeld J, and Luckhoff A.** Role and regulation of TRP channels in neutrophil granulocytes. *Cell Calcium* 33: 533–540, 2003.
20. **Hunter JJ, Shao J, Smutko JS, Dussault BJ, Nagle DL, Woolf EA, Holmgren LM, Moore KJ, and Shyjan AW.** Chromosomal localization and genomic characterization of the mouse melastatin gene (*Mlsn1*). *Genomics* 54: 116–123, 1998.
21. **Jo DG, Jun JI, Chang JW, Hong YM, Song S, Cho DH, Shim SM, Lee HJ, Cho C, Kim do H, and Jung YK.** Calcium binding of ARC mediates regulation of caspase 8 and cell death. *Mol Cell Biol* 24: 9763–9770, 2004.
22. **Jones BE, Lo CR, Liu H, Pradhan Z, Garcia L, Srinivasan A, Valentino KL, and Czaja MJ.** Role of caspases and NF-κB signaling in hydrogen peroxide- and superoxide-induced hepatocyte apoptosis. *Am J Physiol Gastrointest Liver Physiol* 278: G693–G699, 2000.
23. **Kolisek M, Beck A, Fleig A, and Penner R.** Cyclic ADP-ribose and hydrogen peroxide synergize with ADP-ribose in the activation of TRPM2 channels. *Mol Cell* 18: 61–69, 2005.
24. **Kraft R, Grimm C, Grosse K, Hoffmann A, Sauerbruch S, Kettenmann H, Schultz G, and Harteneck C.** Hydrogen peroxide and ADP-ribose induce TRPM2-mediated calcium influx and cation currents in microglia. *Am J Physiol Cell Physiol* 286: C129–C137, 2004.
25. **Kurebayashi N, Harkins AB, and Baylor SM.** Use of fura red as an intracellular calcium indicator in frog skeletal muscle fibers. *Biophys J* 64: 1934–1960, 1993.
26. **Ma S, Ochi H, Cui L, Zhang J, and He W.** Hydrogen peroxide induced down-regulation of CD28 expression of Jurkat cells is associated with a change of site α-specific nuclear factor binding activity and the activation of caspase-3. *Exp Gerontol* 38: 1109–1118, 2003.
27. **McHugh D, Flemming R, Xu SZ, Perraud AL, and Beech DJ.** Critical intracellular Ca^{2+} dependence of transient receptor potential melastatin 2 (TRPM2) cation channel activation. *J Biol Chem* 278: 11002–11006, 2003.
28. **Miller BA, Barber DL, Bell LL, Beattie BK, Zhang MY, Neel BG, Yoakim M, Rothblum LI, and Cheung JY.** Identification of the erythropoietin receptor domain required for calcium channel activation. *J Biol Chem* 274: 20465–20472, 1999.
29. **Montell C.** The TRP superfamily of cation channels. *Sci STKE* 2005: re3, 2005.
30. **Montell C, Birnbaumer L, and Flockerzi V.** The TRP channels, a remarkably functional family. *Cell* 108: 595–598, 2002.
31. **Nagamine K, Kudoh J, Minoshima S, Kawasaki K, Asakawa S, Ito F, and Shimizu N.** Molecular cloning of a novel putative Ca^{2+} channel protein (TRPC7) highly expressed in brain. *Genomics* 54: 124–131, 1998.
32. **Naviaux RK, Costanzi E, Haas M, and Verma IM.** The pCL vector system: rapid production of helper-free, high-titer, recombinant retroviruses. *J Virol* 70: 5701–5705, 1996.
33. **Orrenius S, Zhivotovsky B, and Nicotera P.** Regulation of cell death: the calcium-apoptosis link. *Nat Rev Mol Cell Biol* 4: 552–565, 2003.
34. **Perraud AL, Fleig A, Dunn CA, Bagley LA, Launay P, Schmitz C, Stokes AJ, Zhu Q, Bessman MJ, Penner R, Kinet JP, and Scharenberg AM.** ADP-ribose gating of the calcium-permeable LTRPC2 channel revealed by Nudix motif homology. *Nature* 411: 595–599, 2001.
35. **Perraud AL, Schmitz C, and Scharenberg AM.** TRPM2 Ca^{2+} permeable cation channels: from gene to biological function. *Cell Calcium* 33: 519–531, 2003.
36. **Perraud AL, Takanishi CL, Shen B, Kang S, Smith MK, Schmitz C, Knowles HM, Ferraris D, Li W, Zhang J, Stoddard BL, and Scharenberg AM.** Accumulation of free ADP-ribose from mitochondria mediates oxidative stress-induced gating of TRPM2 cation channels. *J Biol Chem* 280: 6138–6148, 2005.
37. **Pillozzi S, Brizzi MF, Balzi M, Crociani O, Cherubini A, Guasti L, Bartolozzi B, Becchetti A, Wanke E, Bernabei PA, Olivotto M, Pegoraro L, and Arcangeli A.** HERG potassium channels are constitutively expressed in primary human acute myeloid leukemias and regulate cell proliferation of normal and leukemic hemopoietic progenitors. *Leukemia* 16: 1791–1798, 2002.
38. **Prawitt D, Enklaar T, Klemm G, Gartner B, Spangenberg C, Winterpacht A, Higgins M, Pelletier J, and Zabel B.** Identification and characterization of MTR1, a novel gene with homology to melastatin (MLSN1) and the trp gene family located in the BWS-WT2 critical region on chromosome 11p15.5 and showing allele-specific expression. *Hum Mol Genet* 9: 203–216, 2000.
39. **Sano Y, Inamura K, Miyake A, Mochizuki S, Yokoi H, Matsushime H, and Furuichi K.** Immunocyte Ca^{2+} influx system mediated by LTRPC2. *Science* 293: 1327–1330, 2001.
40. **Shirihai O, Attali B, Dagan D, and Merchav S.** Expression of two inward rectifier potassium channels is essential for differentiation of primitive human hematopoietic progenitor cells. *J Cell Physiol* 177: 197–205, 1998.
41. **Steidl U, Bork S, Schaub S, Selbach O, Seres J, Aivado M, Schroeder T, Rohr UP, Fenk R, Kliszewski S, Maercker C, Neubert P, Bornstein SR, Haas HL, Kobbe G, Tenen DG, Haas R, and Kronenwett R.** Primary human CD34+ hematopoietic stem and progenitor cells express functionally active receptors of neuromediators. *Blood* 104: 81–88, 2004.
42. **Tsavaler L, Shapero MH, Morkowski S, and Laus R.** Trp-p8, a novel prostate-specific gene, is up-regulated in prostate cancer and other malignancies and shares high homology with transient receptor potential calcium channel proteins. *Cancer Res* 61: 3760–3769, 2001.
43. **Wehage E, Eisfeld J, Heiner I, Jungling E, Zitt C, and Luckhoff A.** Activation of the cation channel long transient receptor potential channel 2 (LTRPC2) by hydrogen peroxide. A splice variant reveals a mode of activation independent of ADP-ribose. *J Biol Chem* 277: 23150–23156, 2002.
44. **Wu Y and Clusin WT.** Calcium transient alternans in blood-perfused ischemic hearts: observations with fluorescent indicator fura red. *Am J Physiol Heart Circ Physiol* 273: H2161–H2169, 1997.
45. **Zhang MY, Clawson GA, Olivieri NF, Bell LL, Begley CG, and Miller BA.** Expression of SCL is normal in transfusion-dependent Diamond-Blackfan anemia but other bHLH proteins are deficient. *Blood* 90: 2068–2074, 1997.
46. **Zhang MY, Harhaj EW, Bell L, Sun SC, and Miller BA.** Bcl-3 expression and nuclear translocation are induced by granulocyte-macrophage colony-stimulating factor and erythropoietin in proliferating human erythroid precursors. *Blood* 92: 1225–1234, 1998.
47. **Zhang W, Chu X, Tong Q, Cheung JY, Conrad K, Masker K, and Miller BA.** A novel TRPM2 isoform inhibits calcium influx and susceptibility to cell death. *J Biol Chem* 278: 16222–16229, 2003.
48. **Zhuang S, Demirs JT, and Kochevar IE.** p38 Mitogen-activated protein kinase mediates bid cleavage, mitochondrial dysfunction, and caspase-3 activation during apoptosis induced by singlet oxygen but not by hydrogen peroxide. *J Biol Chem* 275: 25939–25948, 2000.